

Supporting Information

Substituted Thiazines as Energy-Rich Analytes for Nonaqueous Redox Flow Cells

^{1,2}Jinhua Huang[‡], ^{2,3}Wentao Duan[‡], ^{1,2}Jingjing Zhang[‡], ^{1,2}Ilya A. Shkrob, ^{2,4}Rajeev S. Assary, ^{1,2}Baofei Pan, ^{1,2}Chen Liao, ^{1,2}Zhengcheng Zhang, ^{2,3,§}Xiaoliang Wei,* ^{1,2}Lu Zhang*

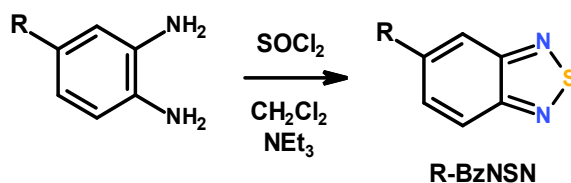
¹Chemical Sciences and Engineering Division, Argonne National Laboratory; ²Joint Center for Energy Storage Research; ³Pacific Northwest National Laboratory; ⁴Materials Science Division, Argonne National Laboratory

[§] Present Address: Indiana University - Purdue University Indianapolis.

Section S1. Materials.

Compound **4** was obtained from Matrix Scientific. DBMMB was obtained as described in ref. 23. All other chemicals were obtained from Aldrich in their purest available form.

To obtain triazinyl derivatives **2**, **3** and **5**, a substituted *o*-phenylenediamine was dissolved in the mixture of dichloromethane and trimethylamine. To this mixture thionyl chloride at 0 °C was added dropwise and then the reaction mixture was refluxed at boiling for 3 h. When cooled down to room temperature, the reaction mixture was washed with water, dried over Na₂SO₄ and then reduced in vacuum to obtain the crude product, which was purified by flash chromatography on silica gel, eluting with ethyl acetate and hexanes (1:2 v/v). See **Figures S1 to S7** for nuclear magnetic resonance spectra.



5-Methyl-benzo[*c*][2,1,3]thiadiazole (2). 3,4-Diaminotoluene (6.11 g, 50 mmol) in 100 mL of dichloromethane, Et₃N (27.8 mL), thionyl chloride (7.29 mL, 100 mmol) yielded **2** (6.45 g, 86%).

¹H NMR (300 MHz, CDCl₃) δ 7.83 (d, *J* = 9.0 Hz, 1H), 7.70 (s, 1H), 7.37 (d, *J* = 9.0, 1H), 2.49 (s, 3H); ¹³C NMR (75 MHz, CDCl₃) δ 155.3, 153.6, 140.0, 132.4, 120.7, 119.8, 21.9.

5-Methoxybenzo[*c*][2,1,3]thiadiazole (3). 4-Methoxy-*o*-phenylenediamine dihydrochloride (4.64 g, 22 mmol) in 50 mL of dichloromethane, Et₃N (18.4 mL), thionyl chloride (3.21 mL, 44 mmol) yielded **3** (2.57 g, 70%).

¹H NMR (300 MHz, CDCl₃) δ 7.83 (dd, *J* = 9.5, 0.5 Hz, 1H), 7.28 (dd, *J* = 9.5, 2.5 Hz, 1H), 7.19 (d, *J* = 2.4 Hz, 1H), 3.92 (s, 3H). ¹³C NMR (75 MHz, CDCl₃) δ 161.3, 156.1, 151.2, 125.4, 121.6, 97.8, 55.8.

5-(Trifluoromethyl)benzo[*c*][2,1,3]thiadiazole (5). 4-(Trifluoromethyl)-*o*-phenylenediamine (4.93 g, 28 mmol) in 60 mL of dichloromethane, Et₃N (15.6 mL), thionyl chloride (4.08 mL, 56 mmol) yielded **5** (4.50 g, 79%).

¹H NMR (300 MHz, CDCl₃) δ 8.35 (dt, *J* = 1.8, 0.9 Hz, 1H), 8.15-8.12 (m, 1H), 7.76 (dd, *J* = 9.2, 1.7 Hz, 1H); ¹³C NMR (75 MHz, CDCl₃) δ 155.5, 153.5, 131.5 (q, *J* = 32.8 Hz), 125.1 (q, *J* = 2.8 Hz), 123.6 (q, *J* = 272.8 Hz), 122.8, 119.80 (q, *J* = 4.8 Hz).

S2. Electrochemical oxidation, cyclic voltammetry, and electron paramagnetic resonance measurements.

Our electrolysis setup included a static H cell (G. Finkenbeiner, Inc., Waltham, MA) with a reticulated vitreous carbon (Duocel, 5 mm x 5 mm cross section) working and counter electrodes and an Ag/AgNO₃ (10 mM in MeCN) reference electrode. This H cell was equipped with a 2 mm thick ceramic separator with P5 frit. Each cell compartment contained 5 mL of 50 mM ROM solutions (1:1 equiv. anolyte + catholyte) in acetonitrile containing 0.5 M LiTFSI (lithium bistriflimide). The charging of these ROMs was controlled using a CHI760D electrochemical workstation (CH Instruments, Bee Cave, TX) operating in the galvanostatic mode. The cell was charged to 100% of the calculated theoretical value at a rate of 5C; the cell fluids were vigorously stirred with a magnetic bar during the electrolysis. The same cell was used to assess the cycling stability of ROMs under galvanostatic cycling at 50% state-of-charge and a rate of 3C. The cathode potential was controlled between -2.5 V and 0 V vs. Ag/Ag⁺ during these cycling tests. In these static experiments for the cells containing **1**, **2**, **3** and **4**, 10% capacity fade was attained after 309, 20, 39, and 26 cycles, respectively. The same cell was also used to obtain cyclic voltammograms. For **Figures 2 and 3** the redox potentials were determined in 5 mM ROM solutions (with a vitreous carbon working electrode and a platinum wire counter electrode) and 5 mM ferrocene was used for additional referencing.

Electrochemically generated radical ions in the cell fluids were observed using continuous-wave (cw) electron paramagnetic resonance (EPR) spectroscopy in the X-band using 100 kHz field modulation (0.2 G, 2 mW). Decay kinetics were obtained at 25 °C by double integration of these cw EPR spectra. The decay kinetics were first order and the half-decay lifetimes were found from the least squares exponential fits, as shown in **Figure S9**. Charged fluids were placed into capillaries that were contained in glass tubes sealed with a Teflon piston seal. All these operations were carried out in an argon filled glove box.

S3. Flow cell tests.

Flow cell tests in **Figure 4** were assembled with graphite felt electrodes (SGL Group, Wiesbaden, Germany) at both sides with a porous separator placed between them. The active size was 1 cm × 5 cm. The electrolytes flowed through the electrodes at a rate of 20 mL/min using a Masterflex L/S peristaltic pump (Cole-Parmer, Vernon Hills, IL). Galvanostatic charge/discharge cycling was performed using a LANHE battery tester (Wuhan LAND Electronics, China). The specific energy density was calculated based on the experimental energy output divided by the total volume of the electrolytes in the cell compartments. Porous polyethylene/silica separators (800 μm thick, pore size 0.15 μm, porosity 57%) were obtained from Daramic LLC (Owensboro, KY). All separators were dried in vacuum at 70°C for 24 h before use. For most cycling, a charging rate of 10 mA/cm² was used.

Figure S10 shows the coulomb, energy, and voltaic efficiencies for the cells shown in **Figure 4**; these plots are similar for all R-BzNSN derivatives. **Figure S11** shows the results for a 100-cycle test for **1**, **2** and **4**, including the capacity fade and cell efficiencies. It is seen that the trends observed in our 50-cycle tests were also observed in these 100-cycle tests.

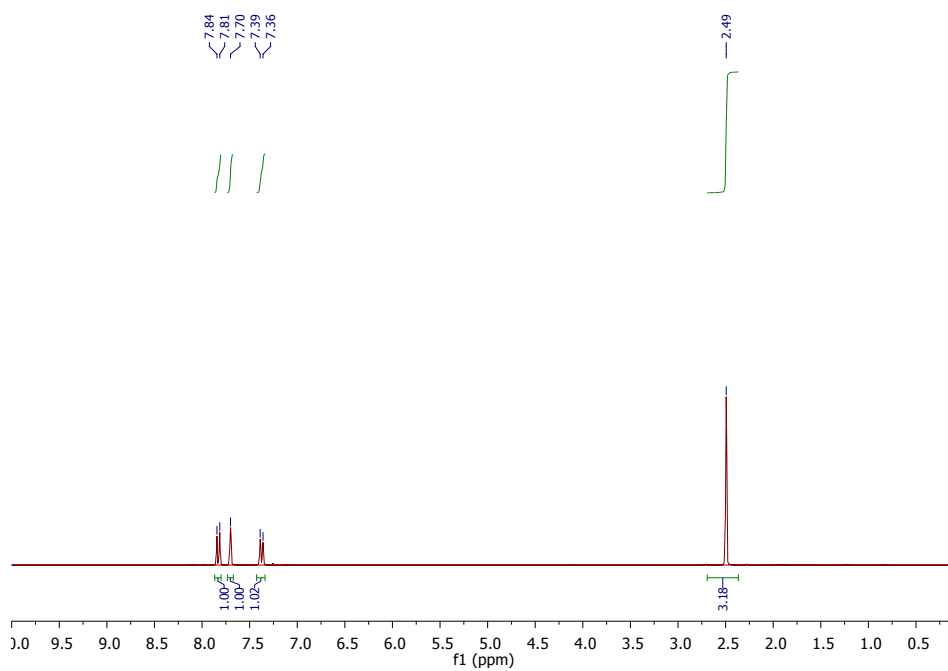


Figure S1. ^1H NMR spectrum of **2** in CDCl_3 .

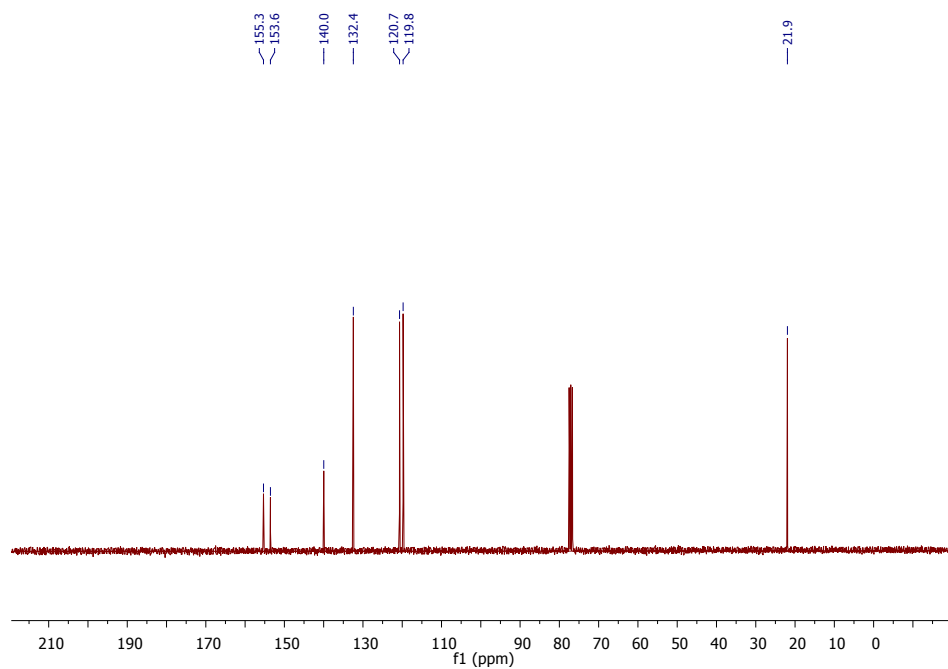


Figure S2. ^{13}C NMR spectrum of **2** in CDCl_3 .

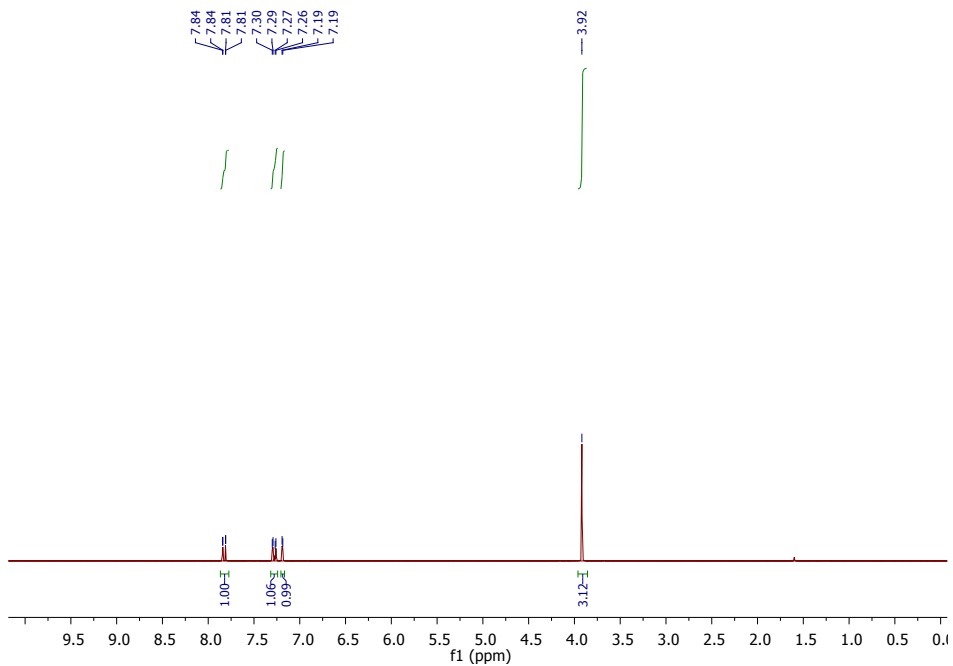


Figure S3. ^1H NMR spectrum of **3** in CDCl_3 .

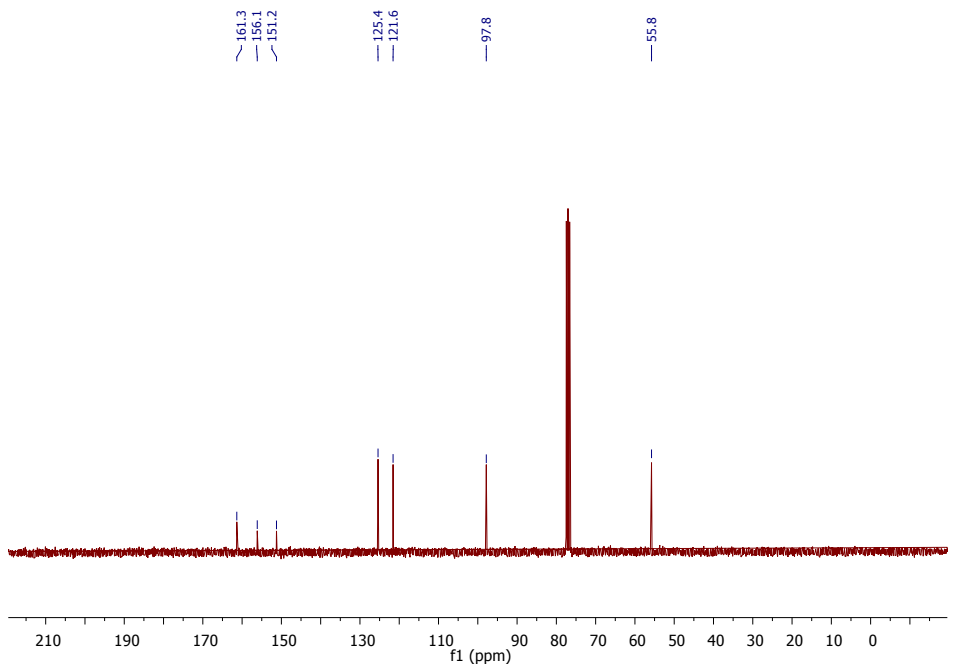


Figure S4. ^{13}C NMR spectrum of **3** in CDCl_3 .

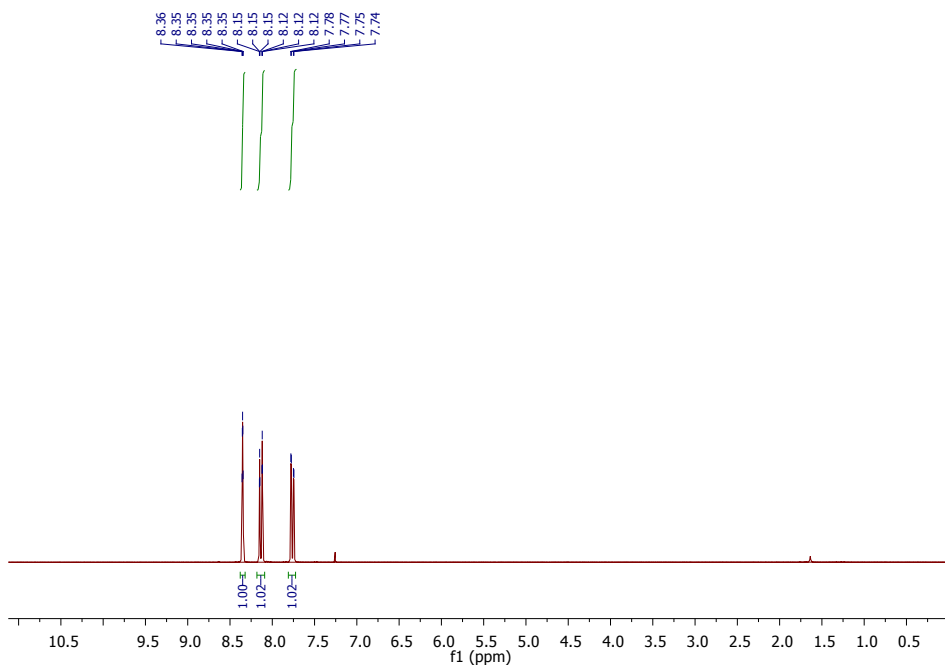


Figure S5. ^1H NMR spectrum of **5** in CDCl_3 .

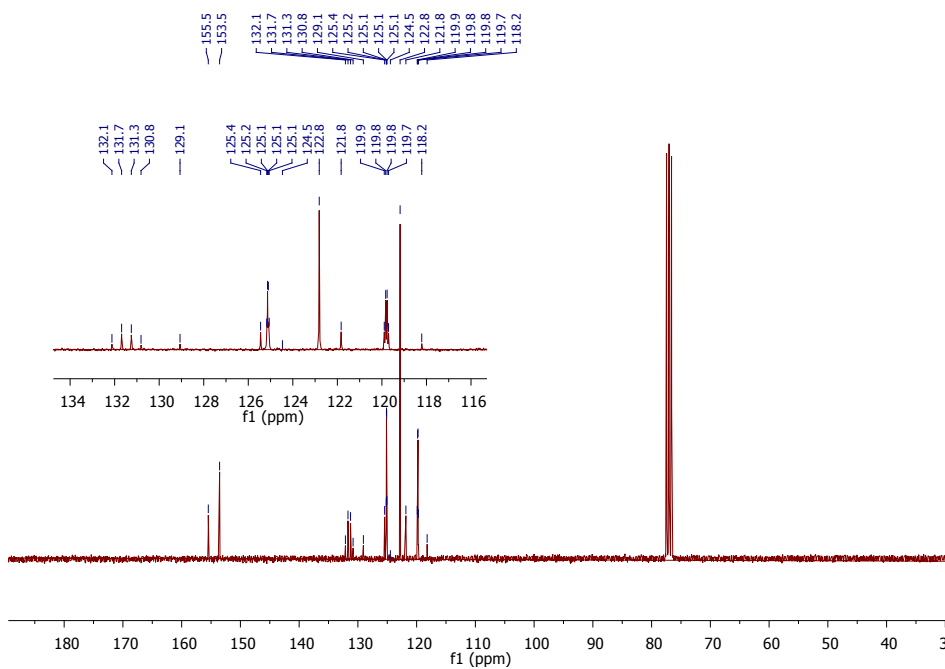


Figure S6. ^{13}C NMR spectrum of **5** in CDCl_3 .

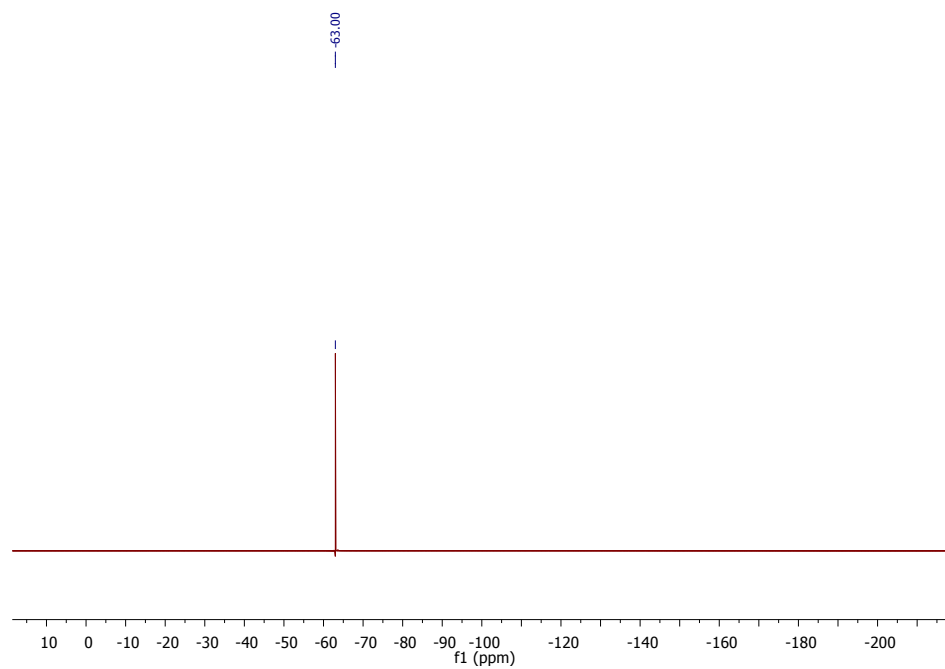


Figure S7. ^{19}F NMR spectrum of **5** in CDCl_3 .

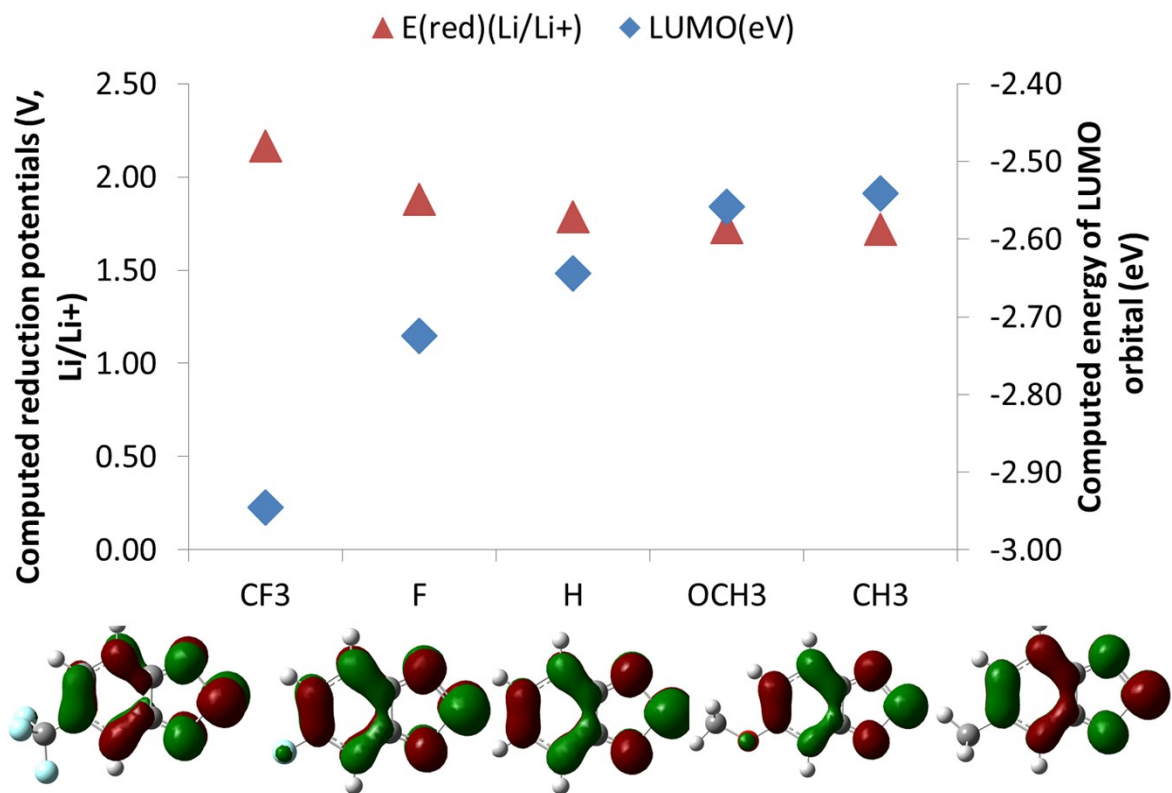


Figure S8. The computed reduction potentials (V vs. Li/Li⁺) and LUMO (lowest unoccupied molecular orbital; *shown below*) energies for several 5-substituted BzNSN derivatives. Density functional theory computations were performed using the B3LYP/6-31+G(d) functional and basis set, respectively, from the Gaussian 09. All geometries are optimized in the acetonitrile solvent, which is modelled using SMD solvation model. When the electron withdrawing groups are introduced, the electron affinity increases, and the analyte molecules exhibit higher reduction potentials.

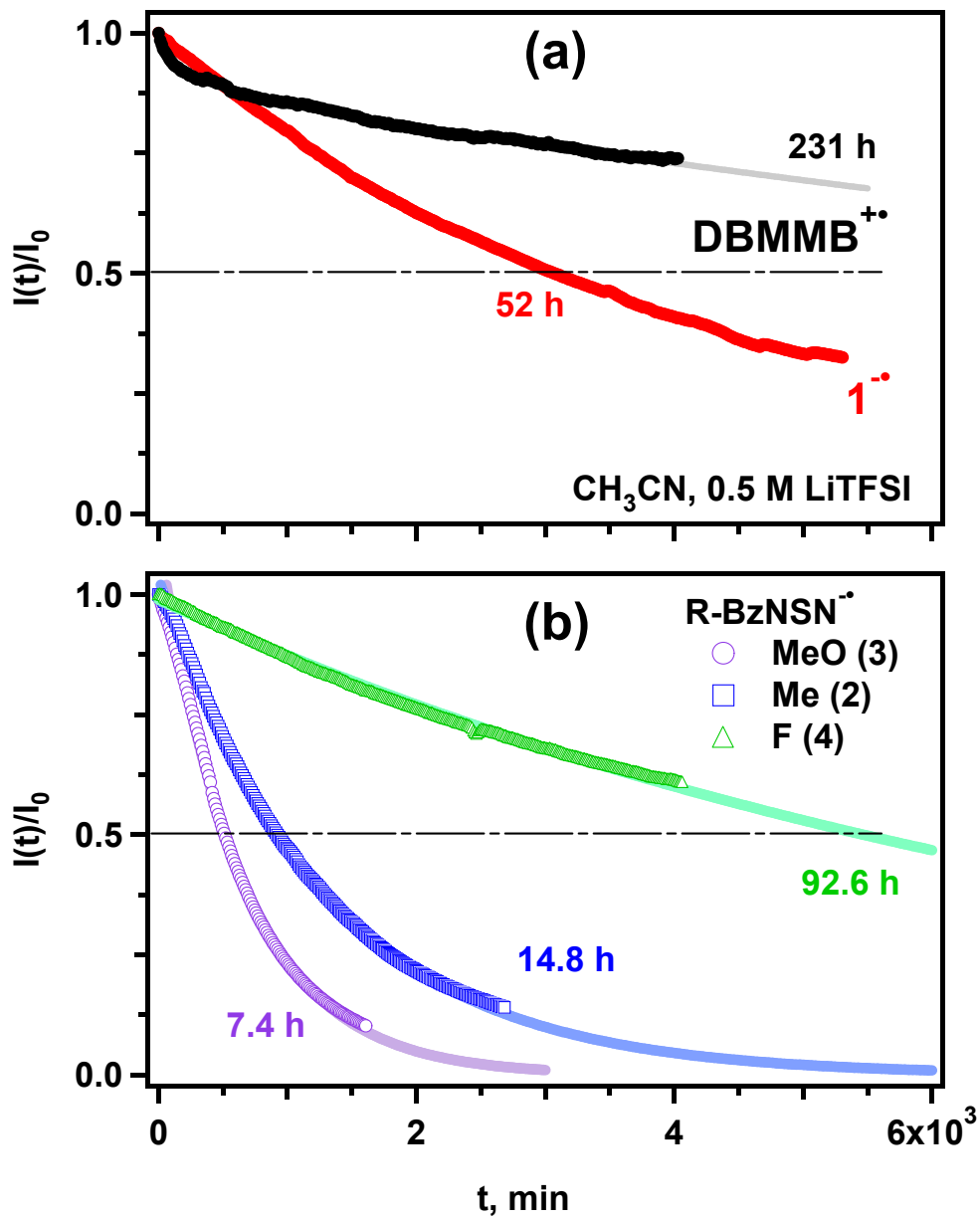


Figure S9. Symbols: normalized decay kinetics of integrated EPR signals ($I(t)$) over time t , for (a) $\text{DBMMB}^{+\bullet}$ radical cation and $1^{\bullet\bullet}$, and (b) $2^{\bullet\bullet}$, $3^{\bullet\bullet}$, and $4^{\bullet\bullet}$ in solutions containing 50 mM ROM each after full charging of the solution (0.5 M LiTFSI in acetonitrile, 25 °C). The solid lines are the least squares first order fits; $t_{1/2}$ times are indicated in the plot. See also **Figure 3** in the text.

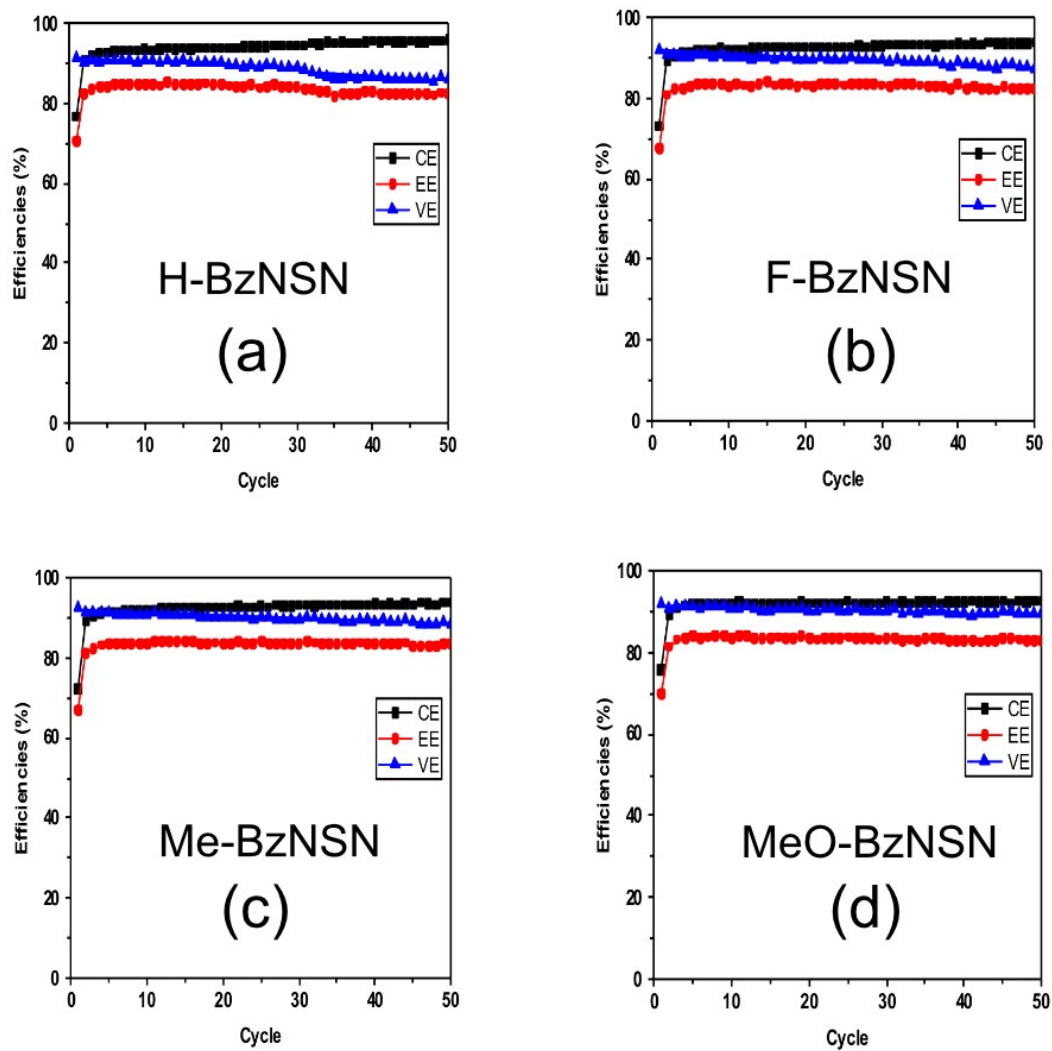


Figure S10. Coulombic (CE), energy (EC), and voltaic (VE) efficiencies for flow cell tests shown in **Figure 4** for (a) **1**, (b) **4**, (c) **2**, and (d) **3**. The substituting groups are indicated in the plot.

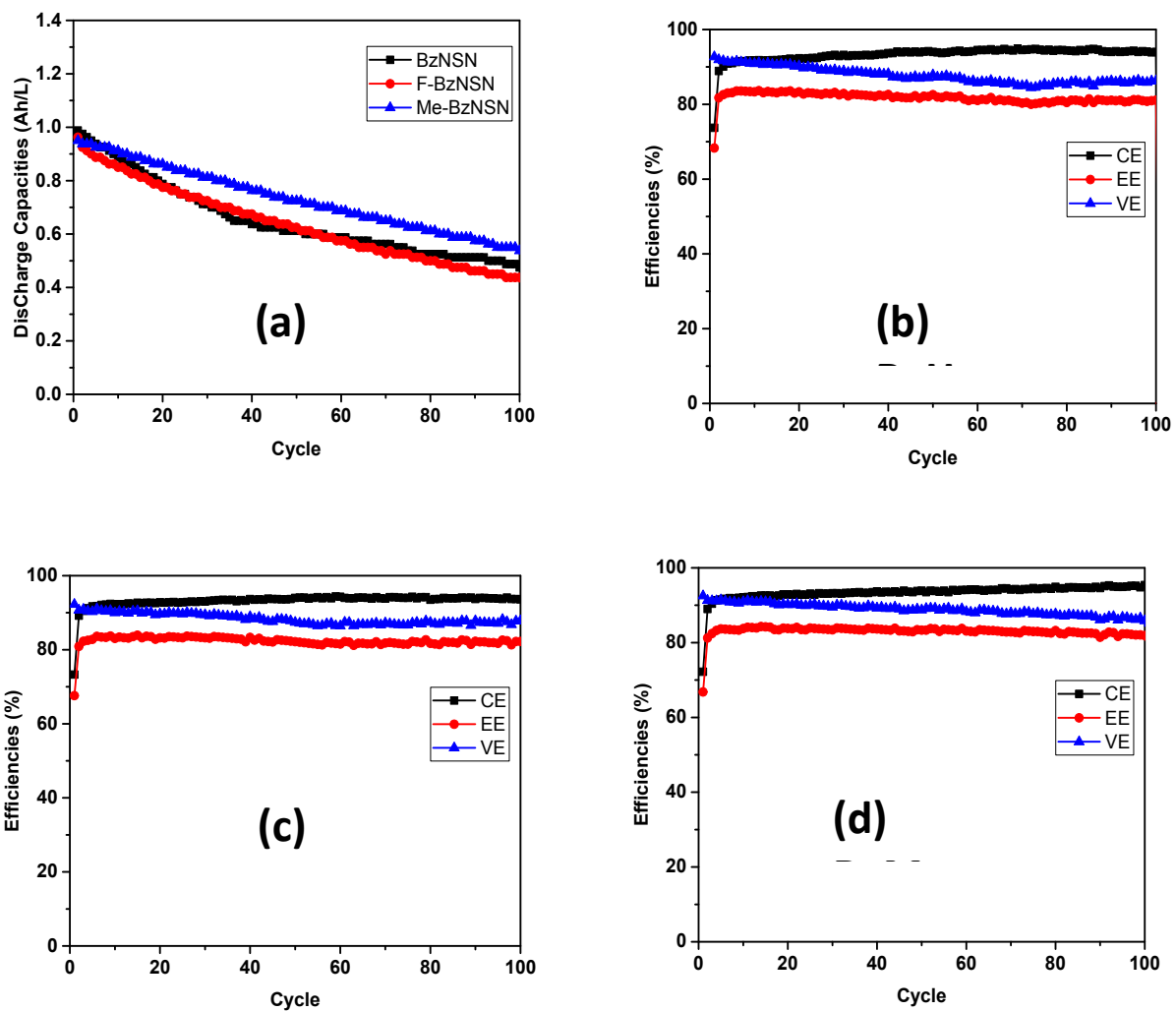


Figure S11. (a) Discharge capacities for the flow cells containing **1**, **2** and **4** analytes for a 100-cycle test (see the inset in panel a for color coding). (b-d) Coulombic (CE), energy (EC), and voltaic (VE) efficiencies for the same three cells, respectively. The same ROM concentrations and conditions were used as in **Figure 4**.

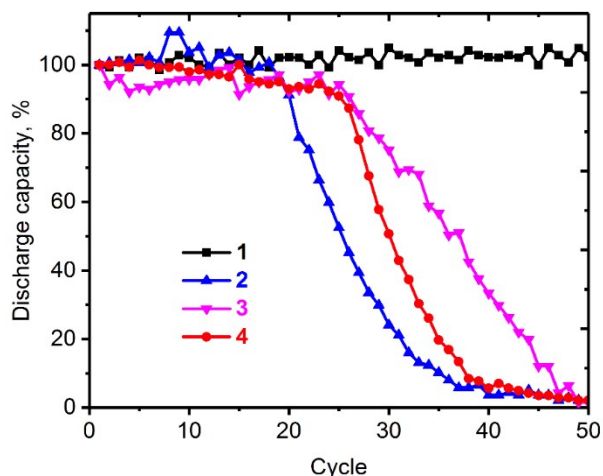
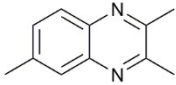
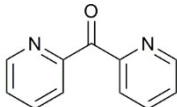
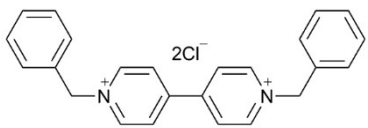
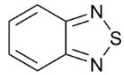


Figure S12. Normalized capacity retention profiles of H cells containing mixed ROMs (50 mM each) in 0.5 M LiTFSI/MeCN (5 ml in each chamber). Those cells were cycled at 3C (20 mA) for 50 cycles and were charged to 50% SOC.

Table S1. Molecular weight, redox potential, and solubility of the quinoxaline,¹ dipyriddyketone,² viologen² and benzothiadiazole analytes for nonaqueous redox flow batteries.

Anolyte	Molecular weight (g/mol)	Redox potential (V vs. Li/Li ⁺)	Solubility
	172.23	~2.64	~7 M in propylene carbonate
	184.19	~2.10	N/A
	409.35	~2.25, ~2.6	N/A
	136.17	~1.46	> 2 M in acetonitrile

References

- Brushett, F. R.; Vaughey, J. T.; Jansen, A. N., An All-Organic Non-aqueous Lithium-Ion Redox Flow Battery. *Adv. Energy Mater.* **2012**, 2 (11), 1390-1396.
- Jansen, A. N.; Vaughey, J. T.; Chen, Z.; Zhang, L.; Brushett, F. R. *U.S. Patent Appl.* 20130224538, 2013